

# Credal Networks for Hazard Assessment of Debris Flows

A. ANTONUCCI<sup>1</sup>, A. SALVETTI<sup>2</sup>, AND M. ZAFFALON<sup>3</sup>

## 1.1 Introduction

Debris flows are among the most dangerous and destructive natural hazards that affect human life, buildings, and infrastructures. Worldwide, these phenomena claim hundreds of lives and millions of dollars in property losses every year.

Starting from the '70s significant scientific and engineering advances in the understanding of the processes and in the recognition of debris flow potential have been achieved (for a review see Costa and Wieczorek 1987; Iverson et al. 1997). Several experiments have been conducted in many laboratories with the aim to investigate the processes of generation, motion and deposition of debris flows. Similarly, field investigation focused on geologic and topographic characteristics of the source areas and, finally, the triggering variables (e.g., rainfall depth and intensity) have been analyzed in order to derive semi-empirical threshold values able to statistically describe debris flow initiation. Takahashi (1991) was the first to propose a comprehensive theory behind the mechanism of debris flow dynamics (Sec. 1.2.1).

Despite these advances, it is widely recognized that human expertise is still a fundamental building block of hazard identification and hazard map construction. This is so in part because many aspects of the whole process are still poorly understood, and because the identification of model parameters is exposed in practice to high uncertainty making it difficult to apply models. In order to close the gap between theory and practice it seems necessary to merge theoretical models with qualitative human knowledge, and to recognize that uncertainty is a pervasive com-

---

<sup>1</sup>IDSIA (“Dalle Molle” Institute for Artificial Intelligence), Galleria 2, CH-6928 Manno (Lugano), Switzerland (alessandro@idsia.ch).

<sup>2</sup>IST (Institute of Earth Sciences), Via Trevano, CH-6952 Canobbio, Switzerland (andrea.salvetti@supsi.ch).

<sup>3</sup>IDSIA (“Dalle Molle” Institute for Artificial Intelligence), Galleria 2, CH-6928 Manno (Lugano), Switzerland (zaffalon@idsia.ch).

ponent of the phenomena under study. It is also particularly important to identify a framework for credibly dealing with uncertainty that is flexible enough to cope with complex scenarios and different sources of information, such as theoretical models, historical data, and expert assessment. We identify this framework with *credal networks* (Cozman 2000a), an imprecise probability model that extends *Bayesian networks* (Pearl 1988) to manage sets of probability mass functions (see Sec. 1.2.2). *Imprecise probability* (Walley 1991) is a very general theory of uncertainty that measures chance and uncertainty without sharp numerical probabilities, and that is founded on rationality criteria similar to the Bayesian theory (see Walley 1996b and de Cooman and Zaffalon 2003, Sec. 2, for gentle introductions to the theory).

This paper presents a credal network model developed to characterize the debris flow hazard in the Ticino canton, southern Switzerland. The model is based on the qualitative representation of causal knowledge and on imprecise-probability quantifications of uncertainty. The causal structure is represented by a directed graph, connecting the triggering factors for debris flows, which we drew on the basis of literature results and domain expertise (Sec. 1.3.1). Section 1.3.2 describes the quantification of uncertainty by probability intervals, showing how intervals are obtained from historical data, expert knowledge, and physical theories about debris flows. The advantages of using intervals here are twofold. When inference of probabilities from data is concerned, probability intervals allow us to carefully deal with the problem of modelling prior ignorance, producing credible posterior estimates (see the description of the *imprecise Dirichlet model* in Sec. 1.2.2). When the problem is to turn expert's knowledge into probabilistic assessments, probability intervals provide quite a flexible modelling tool, not forcing an expert to express knowledge by precise numbers. Overall, credal networks allows us to represent theoretical and empirical knowledge coherently as a single model of debris flow hazard. We are not aware of other models of debris flows hazard with this characteristic.

The primary aim of a model like the one presented in this paper is to support experts in the prediction of dangerous events of debris flow. We have made preliminary tests in this sense by evaluating the predictions of the model on a set of historical cases of debris flows happened in the Ticino canton. The case studies highlight the good capabilities of the model: for all the areas the model produces significant probabilities of hazard. We make a critical discussion of the results in Section 1.5, showing how the results are largely acceptable by a domain expert, and suggesting lines for further sophistication of the proposed model. The positive performance of the model will have to be confirmed by further analysis in the direction

of putting the model to work in practice. However, the evidence already supports the proposed approach as a promising way to play a significant role in the modelling of complex phenomena such as debris flow initiation.

## 1.2 Background

### 1.2.1 Debris Flows

#### Initiation

Debris flows are composed of a mixture of water and sediment. Debris flow events happen because of some natural forces that destroy the structure of the soil and sustain the particles dispersed in the flow, which were originally part of a stable mass on a gully bed or on a basin slope.

Three types of debris flow initiation are relevant. The first type is due to erosion of a channel bed. As a consequence of intense rainfall, surface runoff appears on a steep channel bed, in which a large amount of material was accumulated; the water destabilizes and entrains the debris available to form the debris flow. The second type of initiation is due to landslide: the slid soil mass transforms into debris flow. The third type is the destruction of natural dams. A previous landslide, which dams up a creek, is suddenly destroyed by the water overtopping the dam, which abruptly collapses.

The mechanism to disperse the materials in flow depends on the properties of the materials (grain size, friction angle), channel slope, flow rate and water depth, particle concentration, etc., and, consequently, the behavior of flow is also various.

#### Triggering Factors

According to Costa (1984) prerequisite conditions for most debris flows include an abundant source of unconsolidated fine-grained rock and soil debris, steep slopes, a large but intermittent source of moisture (rainfall or snowmelt), and sparse vegetation.

Rainfall triggering of debris flows and other landslides in steep terrain has been intensively studied. Investigations have included the estimation of empirical relationships between debris flow occurrence and rainfall intensities and durations (e.g., Caine 1980; Cannon and Ellen 1985) and deterministic assessments of the hydrologic processes involved (e.g., Campbell 1975; Johnson and Sitar 1990; Wilson and

Wieczorek 1995).

### Debris Flow Mobilization Mechanisms

Several hypotheses have been formulated to explain mobilization of debris flows. The models generally focus on failure and mobilization of an infinite slope of homogeneous, isotropic soil. Mobilization hypotheses generally start from the assumption that the soil contains sufficient water to saturate the porosity.

The first hypothesis for mobilization derives from the debris flow motion model of Johnson (1984). Takahashi (1981) presented an alternative hypothesis for mobilization, which is part of his model of debris flows, as a water-saturated inertial grain flows governed by the *dispersive stress* concept of Bagnold (1954). Takahashi's model best applies where debris flows mobilize from flash floods that abruptly determine surface-water surcharges in relatively gently sloping, sediment-choked channels. The key role of soil mechanics is emphasized from other hypotheses for debris flow mobilization (e.g., Anderson and Sitar 1995), which underline the role of soil liquefaction caused by increasing pore pressure.

In this study we adopt Takahashi's theory (see Sec. 1.3.2), as the most appropriate to describe debris flow appearance in channel bed with high availability of granular and incoherent material, corresponding to the types of event observed in Switzerland.

#### 1.2.2 Methods

##### Credal Sets and Probability Intervals

In this paper we will restrict the attention to random variables which assume finitely many values (also called *discrete* or *categorical* variables). Denote by  $\mathcal{X}$  the possibility space for a discrete variable  $X$ , with  $x$  a generic element of  $\mathcal{X}$ . Denote by  $P(X)$  the mass function for  $X$  and by  $P(x)$  the probability of  $x \in \mathcal{X}$ . Let a *credal set* be a closed convex set of probability mass functions (Levi 1980).  $\mathcal{P}_X$  denotes a generic credal set for  $X$ . For any event  $\mathcal{X}' \subseteq \mathcal{X}$ , let  $\underline{P}(\mathcal{X}')$  and  $\overline{P}(\mathcal{X}')$  be the *lower and upper probability* of  $\mathcal{X}'$ , respectively. These are defined as follows:

$$\begin{aligned}\underline{P}(\mathcal{X}') &= \min_{P \in \mathcal{P}_X} P(\mathcal{X}') \\ \overline{P}(\mathcal{X}') &= \max_{P \in \mathcal{P}_X} P(\mathcal{X}').\end{aligned}$$

Lower and upper (conditional) expectations are defined similarly. Note that a set of mass functions, its convex hull and its set of *vertices* (also called *extreme mass functions*, i.e. mass functions that cannot be expressed as convex combination of other mass functions in the set) produce the same lower and upper expectations and probabilities.

Conditioning with credal sets is done by element-wise application of Bayes rule. The posterior credal set is the union of all posterior mass functions. Denote by  $\mathcal{P}_X^y$  the set of mass functions  $P(X|Y = y)$ , for generic variables  $X$  and  $Y$ . As far as (conditional) independence is concerned, in this paper we adopt the concept of *strong independence*.<sup>4</sup> Two variables are strongly independent when every vertex in  $\mathcal{P}_{(X,Y)}$  satisfies stochastic independence of  $X$  and  $Y$ , i.e. for every extreme mass function  $P \in \mathcal{P}_{(X,Y)}$ ,  $P(x|y) = P(x)$  and  $P(y|x) = P(y)$  for all  $(x, y) \in \mathcal{X} \times \mathcal{Y}$ . See also Moral and Cano (2002) for a complete account of different strong independence concepts and Cozman (2000b) for a deep analysis of strong independence.

Let  $\mathbb{I}_X = \{\mathbb{I}_x : \mathbb{I}_x = [l_x, u_x], 0 \leq l_x \leq u_x \leq 1, x \in \mathcal{X}\}$  be a set of probability intervals for  $X$ . The credal set originated by  $\mathbb{I}_X$  is  $\{P(X) : P(x) \in \mathbb{I}_x, x \in \mathcal{X}, \sum_{x \in \mathcal{X}} P(x) = 1\}$ .  $\mathbb{I}_X$  is said *reachable* or *coherent* if  $u_{x'} + \sum_{x \in \mathcal{X}, x \neq x'} l_x \leq 1 \leq l_{x'} + \sum_{x \in \mathcal{X}, x \neq x'} u_x$ , for all  $x' \in \mathcal{X}$ .  $\mathbb{I}_X$  is coherent if and only if the related credal set is not empty and the intervals are tight, i.e. for each lower or upper bound in  $\mathbb{I}_X$  there is a mass function in the credal set at which the bound is attained (Campos et al. 1994; Walley 1991).

### The Imprecise Dirichlet Model

Consider a random sample, i.e. a set of values  $x \in \mathcal{X}$  for the discrete random variable  $X$ , drawn independently with chances  $\theta_x$ . The chances  $\theta_x$ , i.e. the parameters of an underlying multinomial distribution, are rarely known in practice, and here we assume that all the information about them is represented by the sample. To approximate the actual chances from the data one can use methods of statistical inference.

The Bayesian approach (Bernardo and Smith 1996) to the statistical inference regards the parameters of an unknown distribution as random variables. The uncertainty about the parameters prior to the availability of the sample is modelled by a density function, called *prior*. This is done also when there is little or no prior knowledge about the chances by using special so-called *noninformative* priors, e.g.

---

<sup>4</sup>Here we follow the terminology introduced by Cozman. Note that other authors use different terms (Couso et al. 2000).

the *uniform* prior. After observing the data, the chosen prior is updated by Bayes theorem to a new density called *posterior*. A parameter of the original unknown distribution can then be approximated by taking its expectation with respect to the posterior. In the case of multinomial samples, the Dirichlet density is the traditional choice for the prior. The Dirichlet  $(s, \mathbf{t})$  density for  $\boldsymbol{\theta}$ , where  $\boldsymbol{\theta}$  is the vector of the chances and  $\mathbf{t}$  is the vector of the  $t_x$  hyperparameters ( $x \in \mathcal{X}$ ), is

$$\boldsymbol{\pi}(\boldsymbol{\theta}) \propto \prod_{x \in \mathcal{X}} \theta_x^{st_x - 1} \quad (1.1)$$

where  $s > 0$ ,  $0 < t_x < 1$  for each  $x \in \mathcal{X}$ ,  $\sum_{x \in \mathcal{X}} t_x = 1$ , and the proportionality constant is determined by the fact that the integral of  $\boldsymbol{\pi}(\boldsymbol{\theta})$  over the simplex of possible values of  $\boldsymbol{\theta}$  is 1. The constant  $s$  is chosen arbitrarily and determines the weight of the prior towards the number of units in the sample. The larger  $s$ , the larger the number of units needed to smooth the effect of the prior information.

The Bayesian approach has great virtues of rationality and coherence, but it is weak when it comes to model prior ignorance. This is recognized to be a very controversial issue (Walley 1991, pp. 226–235), and a possible source of unreliable conclusions. Walley (1996a) has generalized the Bayesian approach by a more objective modelling of prior ignorance, leading to more reliable posterior estimates. According to Walley, prior ignorance should be modelled by *a set* of prior densities. In particular, with multimomial samples, the set is constituted by all the Dirichlet densities obtained by fixing  $s$  in (1.1) and letting the  $t$ -hyperparameters take all the possible values in their domain of definition. The resulting model is called *imprecise Dirichlet model*. By updating the set of priors to a set of posteriors conditional on the data, the model allows posterior inference to be realized similarly to the Bayesian case, with an important difference: the imprecise Dirichlet model leads to lower and upper expectations for a chance. These are achieved by (i) computing the expected value of the chance with respect to the posterior obtained for generic value of  $\mathbf{t}$  and (ii) by minimizing and maximizing this quantity over  $\mathbf{t}$ 's domain of definition.

In summary, in the absence of prior knowledge the imprecise Dirichlet model still produces a reliable posterior estimate for a chance in the form of an interval whose extremes are the above lower and upper expectations. This interval estimate for  $x$  is given by

$$\left[ \frac{\#(x)}{N + s}, \frac{\#(x) + s}{N + s} \right] \quad (1.2)$$

where  $\#(x)$  counts the number of units in the sample in which  $X = x$ ,  $N$  is the total number of units, and  $s$  is like in (1.1). The above lower and upper probabilities can also be interpreted as lower and upper bounds on the relative frequency of  $x$  if we imagine that there are  $s$  hidden observations as well as the  $N$  revealed ones. With the imprecise Dirichlet model,  $s$  is also interpreted as a degree of caution of the inferences and is usually chosen in the interval  $[1, 2]$  (see Walley 1996a for discussion about the value of  $s$ ).

Expression (1.2) permits to infer probability intervals from multinomial samples and hence to infer credal sets, given the relationship between them highlighted in Section 1.2.2. Note that sets of probability intervals obtained using (1.2) are reachable. In this paper all the model probabilities inferred from data will be of the type (1.2).

### Credal Networks

We define credal networks in an incremental way, starting from Bayesian nets. A Bayesian network is a pair composed of a directed acyclic graph and a collection of conditional mass functions. A node in the graph is identified with a random variable  $X_i$  (we use the same symbol to denote them and we also use “node” and “variable” interchangeably). Each node  $X_i$  holds a collection of conditional mass functions  $P(X_i | pa(X_i))$ , one for each possible joint state  $pa(X_i)$  of its direct predecessor nodes (or *parents*)  $Pa(X_i)$ .

Bayesian nets satisfy the *Markov condition*: every variable is independent of its nondescendant non-parents given its parents. From the Markov condition, it follows (Pearl 1988) that the joint mass function  $P(\mathbf{X}) = P(X_1, \dots, X_t)$  over all the  $t$  variables of the net is given by

$$P(x_1, \dots, x_t) = \prod_{i=1}^t P(x_i | pa(X_i)) \quad \forall (x_1, \dots, x_t) \in \times_{i=1}^t \mathcal{X}_i, \quad (1.3)$$

where  $pa(X_i)$  is the assignment to the parents of  $X_i$  consistent with  $(x_1, \dots, x_t)$ .

A credal network is a pair composed of a directed acyclic graph and a collection of conditional credal sets. The graph is intended to code strong dependencies, according to Section 1.2.2: every variable is strongly independent of its nondescendant non-parents given its parents. A generic variable, or node of the graph,  $X_i$  holds the collection of credal sets  $\mathcal{P}_{X_i}^{pa(X_i)}$ , one for each possible joint state  $pa(X_i)$  of its parents  $Pa(X_i)$ . We assume that the credal sets of the net are *separately specified*

(Ferreira da Rocha and Cozman 2002; Walley 1991): this implies that selecting a mass function from a credal set does not influence the possible choices in others. This assumption is natural within a sensitivity-analysis interpretation of credal nets.

Now we can define the *strong extension* (Cozman 2000b), i.e. the set  $\mathcal{P}$  of joint mass functions associated with a credal net:

$$\mathcal{P} = CH \left\{ P(\mathbf{X}) \text{ as from (1.3)} : P(X_i | pa(X_i)) \in \mathcal{P}_{X_i}^{pa(X_i)}, i = 1, \dots, t \right\}$$

where  $CH$  denotes the convex hull operation. In other words,  $\mathcal{P}$  is the convex hull of the set of all the joint mass functions as from (1.3), that are obtained by selecting conditional mass functions from the credal sets of the net in all the possible ways. The expression for the strong extension should make it clear that there is a natural sensitivity analysis interpretation of credal networks: a credal net can be regarded as the set of the Bayesian nets corresponding to the vertices of the strong extension.

### 1.3 The Credal Network

This section details the construction of the proposed model for the hazard assessment of debris flows.

#### 1.3.1 Causal Structure

The key factors responsible for debris flow initiation have been identified in Section 1.2.1. By mind mapping instruments and experts knowledge, the causal relationships among these were analyzed and then expressed by the network in Fig. 1.1. Thirteen nodes are there used to determine the triggering probability of debris, according to its topographic and geological preconditions. The leaf node is the goal of the analysis: it is defined as the depth of debris likely to be transported downstream during a flood event. Such node also represents an integral indicator of the hazard level.

In the following we describe in detail the considerations that led to the causal structure reported in Fig. 1.1. We start by the *geology* node (G). Node G describes the characteristics of the bedrock (*lithology*) in a qualitative way. Rocks are continuously weathered as a result of wind, sun, rain, or frost. Debris flows require a minimum thickness of colluvium (loose, incoherent deposits at the foot of steep slope) for initiation (Reneau et al. 1984). Debris flows occur in colluvium filled bedrock hollows, produced from a variety of bedrock although no clear dependence

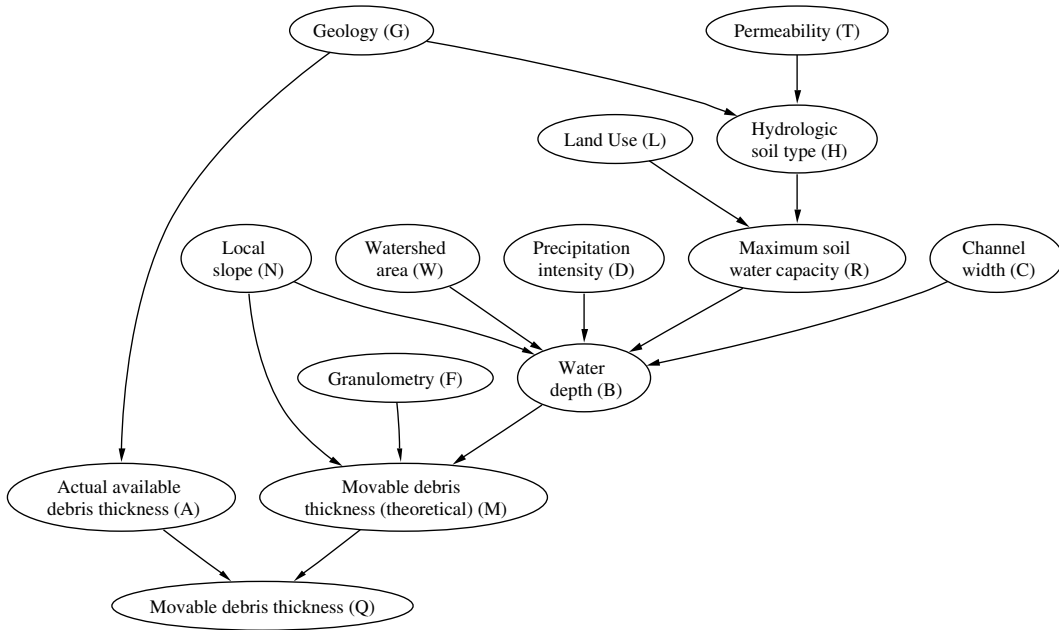


Figure 1.1: The causal structure.

was found between bedrock geology and debris flow occurrence. This observation is considered in the graph with the connection to node A (*actual available debris thickness*) and primarily expresses the propensity of different rocks to produced sediment. Additionally, bedrock properties determine the maximum rate of infiltration and deep percolation, so influencing the generation of surface runoff and the concentration in the drainage network. This influence is accounted for by the connection of the geology to the *hydrologic soil type* (H), which influences the *maximum soil water capacity* (R).

Another important variable is *permeability* (T), i.e. the rate at which fluid can flow through the pores of the soil. If soil has high permeability, rainwater will soak into it easily. If permeability is low, rainwater will tend to accumulate on the surface or flow across the surface if it is not horizontal. The causal relation among geology and permeability determining the different hydrologic soil types was adopted according to the work of Kuntner (2002), who recently used the GEOSTAT infor-

mation system (Kilchenmann et al. 2001) to build a correspondence table between the hydrologic soil groups of the *soil conservation service* infiltration method and the soil of Switzerland. The basic assumption is that soils with high permeability and extreme thickness show a high infiltration capacity, whereas shallow soils with extremely low permeability have a low infiltration capacity.

Another factor that is a significant cause of debris movement is the *land use* (L) cover of the watershed. The land use characterizes the uppermost layer of the soil system and has a definite bearing on infiltration. It describes the watershed cover and usually considers every vegetation type (fallow as well as nonagricultural uses), such as water surfaces, roads, glacier, etc. A forest soil, for example, has a higher infiltration rate than a paved urban area. It is often difficult to precisely assess the role of vegetation on debris flows. Vegetation is also effected by *bedrock type* (G), *slope* (N), and *rainfall* (D), but these influences are too weak in order to be considered into the graph.

Hydrologic soil types were delineated based on information from soil map, geotechnical map and land use map of GEOSTAT. Considering the motivation of the present study, we decided to use the *curve number method* (USDA 1993) to define the infiltration amount of the precipitation, i.e. the maximum soil water capacity (R). The curve number method distinguishes hydrologic soil types which are supposed to show a particular hydrologic behavior. For each land use type there is a corresponding curve number for each hydrologic soil type ( $h_1, \dots, h_4$ ). The infiltration capacity of the soil decreases from  $h_1$  to  $h_4$  (see Tab. 1.3).

The amount of rainfall which cannot infiltrate is considered to accumulate into the drainage network (superficial runoff), increasing the water depth and eventually triggering a debris flow in the river bed. These processes are described by the deterministic part of the graph, related to runoff generation and Takahashi's theory, which take into account topographic and morphologic parameters, such as slope (N) of the source area, *watershed area* (W), *channel width* (C), and *precipitation intensity* (D).

Rivers and torrents adjust their width, depth, and slope to maintain a balance between the water and sediment supplied from upstream, and that exported at the outlet. In this view there exists a link between geology and the intensity of precipitation both influencing the channel width. This influence is still a debated research issue in geomorphology and has therefore been neglected into the graph structure.

The channel width is obviously decisive to determine the water depth, given the

runoff generated within the watershed according to the standard hydraulic assumptions. Field experience in the study region (Ticino canton) indicates that debris flows often start in very steep and narrow creeks, with reduced accumulation area upstream. The complexity and the organization of the channel geometry is therefore usually low and almost similar in the debris flow prone watersheds. For this reasons it was decided to adopt only three categories of channel width. Further physically based analysis of stream geometry based on topographic studies, fractal analysis and network evolution (Rinaldo 1999) are outside the aim of this study.

The climate of the regions in which debris flows are observed is as varied as geology. In addition to the duration and intensity of a storm that ultimately produces a debris flow (rainfall intensity,  $D$ ), the antecedent soil moisture conditions is recognized as an important characteristic. The significant period of antecedent rainfall varies from days to months, depending on local soil characteristics. In this study the peak runoff and the corresponding *water depth* ( $B$ ) in the torrent channel was determined using the mentioned curve number infiltration method and the *rational formula* method.

According to the rational formula, the maximum runoff rate in a catchment is reached when all parts of the watershed are contributing to the outflow. This happens when the time of concentration (the time after which the runoff rate equals the excess rainfall rate) is reached. In the specific case we focused on the identification of areas likely sources of debris flows: it is well known from several observations, that debris flows often occur in different surges and the hydrological components only constitute one of the several variables involved. Furthermore it is widely recognized that the drainage network of small torrents is not univocally defined and highly variable during the flood event. In this perspective topographic variables, like the length of the main channel and the time of concentration, lose the classical meaning assumed in standard hydrological applications. For these reasons fixed rainfall duration (one hour) was defined as critical rainfall interval for further analysis. Therefore the rainfall intensity classes defined for the rainfall node can easily be converted in rainfall depth and corresponding peak discharge. By using the classical river hydraulics theory, the water depth in a channel with uniform flow and given discharge, water slope and roughness coefficient can be determined with the Manning-Strickler formula (see Sec. 1.3.2, and Maidment 1993 as general reference about the Manning-Strickler and the rational formula).

The *granulometry* ( $F$ ), represented by the average particle diameter of the sediment layer, is required to apply Takahashi's theory which describes the debris flow

triggering mechanism. A corresponding node was therefore defined in the graph. Note that the theory needs also the *friction angle*, but no node was created in this case as there exists an empirical one-to-one relationship between granulometry and friction angle. According to the definition of the variables, Takahashi's theory can finally be applied, in order to determine the *theoretical thickness of debris* (M) that could be destabilized by intense rainfall events. The resulting value must be compared with the *actual available debris thickness* (A) in the river bed. The minimum of this two values is the leaf node of the graph (Q), which is a proxy indicator of the debris flow hazard level in the selected channel reach.

### 1.3.2 Quantification

This section reports the quantification of uncertainty for all the variables in the network. Recall that the variables have been discretized (e.g., Tab. 1.1), so quantifying uncertainty means to specify the conditional mass functions  $P(X_i|pa(X_i))$  for all the nodes  $X_i$  and all the possible instances of the parents  $pa(X_i)$ . As stated in the Introduction, we allow the specification to be imprecise, in the sense that each value  $P(x_i|pa(X_i))$  can lie in an interval. The intervals for  $P(x_i|pa(X_i))$  ( $x_i \in \mathcal{X}_i$ ) define a set of mass functions  $\mathcal{P}_{X_i}^{pa(X_i)}$ , according to Section 1.2.2, to which  $P(X_i|pa(X_i))$  belongs.

Let us now consider how the intervals have been determined. In the most informative cases, the conditional distribution express a functional relation and the intervals reduce to a single *degenerate* (i.e. 0-1 valued) mass function. In the other cases, probabilistic knowledge coming from data or the expert is quantified by probability intervals.

### Determinism

Section 1.3.2 outlined a theoretical description of some aspects of the debris flow process. We embed this theoretical background about the nodes B, M and Q and the related parents by degenerate distributions  $P(B|pa(B))$ ,  $P(M|pa(M))$  and  $P(Q|pa(Q))$  for all the joint states of parents (since variables are discrete and the theoretical formulae are stated for continuous values, this has also involved the choice of representative values for all the states of parents).

Table 1.1: Discretization for node Q (the same discretization is used for nodes A and M).

State	Range [cm]
$q_1$	<10
$q_2$	10–50
$q_3$	>50

The theoretical equation regarding the water depth (node B) is<sup>5</sup>

$$b(c, d, n, r, w) = \begin{cases} \frac{k_1 w}{k_2 c^{\frac{5}{3}} \sqrt{\tan n}} \cdot \frac{(d - \frac{r}{20})^2}{(d - \frac{r}{20}) + r} & \text{if } d > \frac{r}{20} \\ 0 & \text{otherwise} \end{cases}$$

where  $k_1 = 0.278$  is a constant and  $k_2 = 25 \sqrt[3]{m}/s$  is the coefficient of bed roughness. The equation follows from Manning-Strickner's formula and the rational formula. Intuitively the formula expresses the proportionality between the water depth  $b$  and the watershed area  $w$ , as well as the decrease of  $b$  for increasing slope  $n$  and channel width  $c$ . The term  $r/20$  reflects water dispersion reducing the effect of the precipitation  $d$ .

Regarding node M, the effect of a water depth  $b$  on the movable quantity  $m$  was quantified by Takahashi as

$$m(b, f, n) = b \left[ k_3 \left( \frac{\tan f}{\tan n} - 1 \right) - 1 \right]^{-1}. \quad (1.4)$$

The relation is linear, with a coefficient taking into account the local slope  $n$  and the internal friction angle  $f$  (which can be obtained from the granulometry, see the end of Sec. 1.3.1) where  $k_3 = C_b(d_b - 1)$ , with  $d_b \simeq 2.65$  the relative density of the grains and  $C_b \simeq .7$  the volumetric concentration of the sediments. We recall that the variables involved in (1.4) must satisfy the constraints

$$1 + \frac{1}{k_3} \leq \frac{\tan f}{\tan n} \leq 1 + \frac{1}{k_3} \cdot \left( 1 + \frac{b}{f'} \right).$$

---

<sup>5</sup>By abusing notation, we will use the same letter for generic values of nodes and the corresponding variable in the theoretical formulae.

If the inequality on the left-hand side is violated, shallow landslides can occur also in absence of water depth, but technically speaking these are not debris flows. If the remaining inequality fails, the movable quantity as in (1.4) is thinner than the granulometry  $f'$  and no flow can be observed.

Equation (1.4) proposes a theoretical value for the movable quantity, which does not take into account how much material is physically available. Of course, the actual movable quantity cannot exceed the available material  $a$ . So, the final relation is given by

$$q(a, m) = \min\{a, m\}.$$

## Data

The GEOSTAT database (Kilchenmann et al. 2001), restricted to the Ticino canton, was used to estimate the mass functions of the nodes H, R, G, T, L and N. The database is operated by the *Swiss Federal Office of Statistics* and contains a federal GIS database of geocoded, spatially relevant data sets coming from various, mostly governmental, sources. Three thematic maps are available: land use raster map, with a grid size of  $100 \times 100$  meters; soil type raster map, containing 144 soil classification units, derived from the combination of typical landscape units and soil characteristics; and a simplified geotechnical raster map, which contains 30 classes characterizing the first geological layer under the soil.

We used the imprecise Dirichlet model (Sec. 1.2.2) to infer probability intervals from GEOSTAT (we used the value 2 for the hyperparameter  $s$ , which is the most cautious choice suggested by Walley). Note that the length of the inferred intervals depends on the number of available records for the estimates, as from (1.2). For example, when no data are available for a given state of a random variable, we obtain maximally imprecise, or *vacuous*,  $[0, 1]$  intervals. In presence of data the lengths decrease and in the limit of a very large amount of data they are nearly precise (we approximate the numbers to the fourth decimal digit). This is the case of the intervals for the root nodes G, T, L and N (e.g., Tab. 1.2), as there is about one million records in the database.

The situation changes for the remaining nodes H and R (e.g., Tab. 1.3). Conditional probabilities are estimated on the basis of the subsets of the database related to the conditioning states of the parents. The available records are thus usually much smaller than one million, for each probability, producing different sizes of intervals. In other words the imprecise Dirichlet model keeps track of the different amount of information carried by data adapting the degree of imprecision, i.e. the

Table 1.2: Precise mass function for the root node G, as inferred from data.

State	Description	$P(g_i)$
$g_1$	Unconsolidated soil	0.1821
$g_2$	Malrs and Conglomerates	0.0014
$g_3$	Limestone	0.0930
$g_4$	Crystilline Rock	0.0043
$g_5$	Porphyry	0.0066
$g_6$	Gneiss	0.7126

length of the intervals, which is something that cannot be done by point probability estimates.

Table 1.3: An imprecise mass function for the node H, as inferred from data.

State	Description	$P(h_i g_2, t_4)$
$h_1$	Low runoff potential	[0.0000, 0.0247]
$h_2$	Moderate infiltration rates	[0.0000, 0.0247]
$h_3$	Low infiltration rates	[0.0988, 0.1235]
$h_4$	High runoff potential	[0.8765, 0.9012]

## Expert

Up to now our quantification process was accomplished under the support of quantitative information (theory and data). Nevertheless some nodes can be quantified only by expert's knowledge. The capability to integrate in the same model quantitative and empirical knowledge is a remarkable feature of the credal network model. The expert expressed the mass functions for W, D, C, F and A, by a collection of intervals for each mass function (see for example Tab. 1.4). On the technical side, we verified coherence of the proposed intervals (Sec. 1.2.2), whence the non-emptiness of the corresponding credal sets.

Table 1.4: Expert's estimates for granulometry.

State	Description [mm]	$P(f_i)$
$f_1$	< 10	[0.01, 0.10]
$f_2$	10–100	[0.10, 0.20]
$f_3$	100–150	[0.25, 0.40]
$f_4$	150–250	[0.25, 0.35]
$f_5$	> 250	[0.12, 0.18]

## 1.4 Algorithmic Issues

Section 1.3 has described our imprecise probability model for hazard assessment of debris flows. In order to use the model in practice, we need algorithms that allow us to work with credal nets. This section illustrates the computational challenges posed by credal networks and the solution implemented here. We focus on the task called *updating*, which is one of the most popular computations with Bayesian and credal networks.

Let  $E$  be a vector of variables of the credal network, and let  $e$  denote an observed state of  $E$ .  $E$  is also called the vector of *evidence variables*, and  $e$  is called *evidence*. Consider any node  $X$  not in  $E$ . The updating corresponds to compute the posterior probability  $P(X|E = e)$  with Bayesian nets, and the lower and upper posterior probabilities  $\underline{P}(X|E = e)$  and  $\overline{P}(X|E = e)$ , with credal networks.

The updating is intended to update our prior beliefs about  $X$  to posterior beliefs given a certain evidence  $E = e$ . It is important to stress a methodological point here: the updating represents the correct way to update beliefs if and only if the unobserved network variables are *missing at random* (Grunwald and Halpern 2003), which roughly means that variables cannot be missing in a systematic way. This point is quite delicate as the failure of the missing-at-random assumption can lead the updating to produce highly misleading results. The present work assumes that observations are missing at random as this seems to be a reasonable approximation to the typical way the evidence about hazard areas is collected in the Ticino canton.

From the computational point of view, the updating problem with credal nets is *NP-hard* (Ferreira da Rocha and Cozman 2002) also when the graph is a polytree (for a review of updating algorithms with credal nets see Cano and Moral 1999). A polytree is a directed graph with the characteristic that forgetting the direction

of arcs, the resulting graph has no cycles. Contrast the situation with Bayesian nets, for which the updating takes linear time in the same conditions. The hardness result is related in some way to the fact that strong extensions can have a very large number of extreme mass functions.

Indeed, the updating can be computed in principle by (i) exhaustively enumerating the vertices  $P_k$  of the strong extension; and by (ii) minimizing and maximizing  $P_k(X|E = e)$  over  $k$ , where  $P_k(X|E = e)$  can be computed by any updating algorithm for Bayesian networks (recall that each vertex of the strong extension is a Bayesian network). The exhaustive approach is attractive because it is conceptually very easy, but it is often not viable due to the large number of vertices of the strong extension. The present work is a nice exception to the rule, as the type of network, jointly with the way evidence is collected, make the exhaustive approach viable in reasonable times. In practice, we make the above steps (i–ii) along the lines used to define the strong extension in Section 1.2.2: we consider all the possible joint ways to select vertices from the credal sets  $\mathcal{P}_X^{pa(X)}$  (for all nodes  $X$  and all the states of their parents that are consistent with  $E = e$ ); and the second step follows by executing a Bayesian network updating for each joint selection. Note that the exhaustive algorithm needs credal sets be specified via sets of vertices, rather than as probability intervals. This is not a problem as there are well-known algorithms to convert from one representation to the other. To produce extreme mass functions in the present work, we used the software tool *lrs* (<http://cgm.cs.mcgill.ca/~avis/C/lrs.html>) as a preprocessing step of the exhaustive algorithm.

## 1.5 Case Studies

### 1.5.1 Description

The methodology developed in this work has been applied to some case studies concerned with hazardous areas of the Ticino canton, in Switzerland. The empirical study was intended to validate the model in a preliminary way, by evaluating its adequacy in critical setups. This idea led us to choose testing areas that underwent a considerable event of debris flow in the past. The conditions of the areas prior to the event (see Tab. 1.5) have been given as input to the credal network model. This information was extracted from GEOSTAT for geology, land use, watershed area and slope (derived from the original *digital elevation model*). The precipitation intensity, the channel width, the granulometry of the material and the actual available debris

thickness were available in form of an event report. The credal network was expected to predict the hazard on this basis, by indicating that substantial detachment of sediment should be expected with significant probability.

Table 1.5: Details about the case studies. Case 1 happened at Buffaga Creek in the municipality of Ronco sopra Ascona, 28 Aug. 1997. Case 2 at Cumaval Creek in Riva S. Vitale, 2 Jun. 1992. Case 3 at S. Defendente Creek in Capolago, 2 Jun. 1992. Case 4 at Val Creek in Ghirone, 1 Aug. 1998. Case 5 at Cassinello Creek in Claro, 4 Jul. 2000. Case 6 at Foioi Creek in Caveragno, 31 Aug. 1992.

Case	Geology	Landuse	Granulometry [mm]	Precip. [mm/h]	Watershed [km <sup>2</sup> ]	Slope [deg]	Channel [m]	Avail. [m]
1	Gneiss	Forest	10–100	100	0.26	38	4	1.0–1.5
2	Porphyry	Forest	< 10	70	0.32	35	6	1.0–1.5
3	Limestone	Forest	< 10	70	0.06	35	4	0.7–1.0
4	Gneiss	Unprod. veg.	100–150	30	0.11	40	8	> 1.5
5	Gneiss	Forest	< 10	50	0.38	30	4	0.7–1.0
6	Gneiss	Bare soil	150–250	30	2.80	30	8	1.0–1.5

## 1.5.2 Results and Discussion

Table 1.6: Posterior probabilities of the states of node Q, i.e. of the movable debris thicknesses, in the six cases considered. The second case presents significantly imprecise probabilities which are written explicitly as intervals.

State	Cases					
	1	2	3	4	5	6
$q_1$	0.0000	[0.0018, 0.0969]	0.0076	0.5628	0.0062	0.5926
$q_2$	0.0055	[0.0048, 0.0636]	0.2764	0.4372	0.9034	0.3677
$q_3$	0.9945	[0.8385, 0.9933]	0.7160	0.0000	0.0904	0.0397

The results of the analysis are listed in Tab. 1.6. The hazard level is identified with the probability of a defined debris thickness to be transported downstream.

In the first three cases the results indicate a high debris flow hazard level in the source area (which corresponds to an instable debris thickness greater than 50 cm,

see Tab. 1.1). High probabilities of state  $q_3$  are in good agreement with historical observations at the Buffaga Creek (case 1) and at the Cumaval Creek (case 2) where channel bed erosion of more than 50 centimeters were extensively observed after the debris flow event. In case 3 (S. Defendente Creek) a non-negligible probability of medium movable debris thickness is also related to the small granulometry, which characterized the watershed. Significant probabilities (about 0.90) of the intermediate state (instable debris thickness between 10 and 50 cm) were obtained for case 5 (Cassinello Creek), due to the gentler bed slope ( $30^\circ$ ) as compared with the other cases. This result is confirmed by data collected during a field campaign after the event: a relatively regular and shallow erosion depth was observed along the channel bed, with only few deeper bed erosion. According to antecedent hazard mapping, geologists did not assign a high debris flow hazard level to the Cassinello Creek and the event was mainly triggered by very intense and concentrate precipitation.

In case 4 (Val Creek) the low hazard prediction can plausibly be explained through some of the assumptions adopted to design the network: (i) in that case the watershed area is very small and the hydrological hypotheses assumed (rational formula and critical duration of one hour, see Sec. 1.3.1) in the network are probably insufficient to explain the processes that triggered the debris flow. Additionally (ii), the observed hourly precipitation was not extreme (30 mm/h); the antecedent soil moisture due to the rainfall of hours and days before, not considered in the graph as a node, played probably a key role in this case and suggests possible further improvements in the graph structure.

In case 6 (Foioi Creek) the probability are decreasing with increasing debris thickness. The evidence is the most extreme out of the six cases: a relatively high upstream area (2.8 km<sup>2</sup>), large channel depth and high medium grain size. These conditions partially explain the results.

As more general comment, it is interesting to observe that in almost all cases posterior probabilities are nearly precise. The conclusions are strong basically because of the strong evidence collected about the cases. Note that in case 6, although the probabilities are significantly imprecise, the results are strong anyway as we can still obtain a single more probable state, namely  $q_3$ . Of course, obtaining strong conclusions from weakly stated probabilistic assumptions increases our confidence about the plausibility of the conclusions.

Now we make a different type of analysis. So far we have assumed that the evidence was precisely available each time, but this is usually an approximation for the grain size of debris material and the channel depth on the source area. This

is not related to our empirical study only; it is a general problem that affects the application of models of hazard of debris flows, and that limits the real application of physical theories, such as Takahashi's theory for example.

We focus on grain size. We wonder whether we can draw credible conclusions in case 6 for which the observation of grain size is uncertain. From the historical event report, we can exclude that node  $F$  was in state  $f_1$  or  $f_2$ . There are chances that  $f_4$  was the actual state ( $f_4$  is the evidence used in the preceding experiments for  $F$ ), but this cannot definitely be established. In order to study the sensitivity of the results with respect to grain size, we take the most conservative position of letting the states  $f_3$ ,  $f_4$  and  $f_5$  be all plausible evidences. Table 1.7 shows the posterior mass functions for node  $Q$  obtained by separately considering the values  $f_3$ ,  $f_4$  and  $f_5$  for node  $F$  in the evidence. An important conclusion, robust to the uncertain observation of grain size, is that the most dangerous event of debris flow ( $q_3$ ) is very improbable. On the other hand, we cannot establish whether or not some debris flow should be expected; depending on the grain size,  $q_1$  is much more probable than  $q_2$  and vice versa. As expected, the hazard is very sensitive to the actual grain size.

These results are of major importance as they allow the user to indirectly assess the importance of observations. The sketched method could be used, depending of the required level of accuracy, to decide if additionally field campaigns are needed to collect other data or if the obtained results are satisfactory for hazard estimation.

It is interesting to see what conclusions can be drawn when no observation at all is made about granulometry. Table 1.8 reports the posterior mass function for  $Q$  obtained without instantiating  $F$ . The conclusions are nearly the same. This emphasizes the critical role played by granulometry for debris flow hazard assessment.

Table 1.7: Posterior probabilities of the states of node  $Q$  with the same evidences of the case 6, except for the node  $F$ , with three different values.

State	$f_3$	$f_4$	$f_5$
$q_1$	0.0122	0.5926	0.9603
$q_2$	0.9481	0.3677	0.0000
$q_3$	0.0397	0.0397	0.0397

Table 1.8: Posterior probabilities of the states of node  $Q$  with the same evidences of the case 6, except for node  $F$  that is not instantiated.

State	$P(q_i e)$
$q_1$	[0.2703, 0.5270]
$q_2$	[0.4297, 0.6785]
$q_2$	[0.0434, 0.1132]

## 1.6 Conclusions

We have presented a model for determining the hazard of debris flows based on credal networks. Credal networks present several advantages for this application. Besides providing a graphical language for modelling cause-effect relationships at the physical level, they make it possible to credibly deal with qualitative uncertainty and, through the imprecise Dirichlet model, with robust inference from data. These characteristics, in turn, favor obtaining credible conclusions, which are a primary objective for this type of application.

The presented model has been developed for the Ticino canton, in Switzerland. Extension to other areas is possible by re-estimating the mass functions obtained from data and expert's knowledge, which have local nature. In fact, the graphical structure represents causal knowledge that can reasonably be regarded as independent of the geographical area, and the same can be said about the physical theories incorporated in the network (but recall that Takahashi's theory is best suited to describe debris flows that appear on steep channel beds, so different theories might be worth considering in other cases). Another point that should seriously be taken into account moving to a different context is the assumption that the network variables are missing at random. In this were not the case, further considerations should be made (de Cooman and Zaffalon 2003).

Computational issues might also be relevant when moving to another environment. In the present case, the updating was computed in less than one hour, in the worst case, on a 2.8 GHz Pentium 4 machine. Such easy computation depends on the nice interplay of the network structure and the way evidence is typically collected in the Ticino canton. In other geographical regions where the evidence is collected differently, it could be necessary to consider solution methods other than the exhaustive approach (Sec. 1.4). Among those, the *branch and bound* method of Ferreira da Rocha et al. (2003) is promising and worth considering.

There are many possible improvements of the presented model that could be pursued in the future. These include the sophistication of the model to include further triggering factors as highlighted by the case studies; the treatment of continuous variables in the network, in order to avoid the loss of information introduced by discretizations; the study of different methods of inference in the network to determine the environmental conditions that should be avoided in order to prevent debris flows; and, perhaps most importantly, an extensive empirical study to validate the model under a variety of conditions, which is a pre-requisite to put the model to work in practice.

Debris flows are a serious problem, and developing formal models can greatly help us avoiding their serious consequences. The encouraging evidence provided in this paper makes credal networks to be models worthy of further investigation in this respect.

## Acknowledgements

The authors would like to thank the Swiss Federal Office of Topography for providing the digital elevation model, and the Swiss Federal Statistical Office for the landuse, soil suitability, and geotechnical maps. Bayesian network updating has been computed by the software *SMILE*, developed at the Decision Systems Laboratory of the University of Pittsburgh. Extreme mass functions have been obtained by D. Avis' vertex enumeration software *lrs*. The authors of these public software tools are gratefully acknowledged. This research was partially supported by the Swiss NSF grant 2100-067961.02.

## Bibliography

- Anderson, S. A. and N. Sitar (1995). Shear strength and slope stability in a shallow clayey soil regolith. *Reviews in engineering geology* 10, 1–11.
- Bagnold, R. A. (1954). *The physics of blown sand and desert dunes*. New York: William Morrow and Co.
- Bernardo, J. M. and A. F. M. Smith (1996). *Bayesian Theory*. New York: Wiley.
- Caine, N. (1980). The rainfall intensity-duration control of shallow landslides and debris flows. *Geogr. Ann.* A62, 23–27.

- Campbell, R. H. (1975). Soil slips, debris flows, and rainstorms in the Santa Monica Mountains and vicinity, Southern California. *US Geol. Surv. Prof. Pap.* 851.
- Campos, L., J. Huete, and S. Moral (1994). Probability intervals: a tool for uncertain reasoning. *International Journal of Uncertainty, Fuzziness and Knowledge-Based Systems* 2(2), 167–196.
- Cannon, S. H. and S. Ellen (1985). Rainfall conditions for abundant debris avalanches, San Francisco Bay Region, California. *Calif. Geol.* 38, 267–272.
- Cano, A. and S. Moral (1999). A review of propagation algorithms for imprecise probabilities. In (*de Cooman, Cozman, Moral, and Walley 1999*), pp. 51–60.
- Costa, J. E. (1984). *Physical geomorphology of debris flows*, Chapter 9, pp. 268–317. Berlin: Costa, J. E. and Fleisher, P. J. - Springer-Verlag.
- Costa, J. H. and G. F. Wieczorek (1987). *Debris Flows/Avalanches: Process, Recognition and Mitigation*, Volume 7. Boulder, CO: Geol. Soc. Am. Reviews in Engineering Geology.
- Couso, I., S. Moral, and P. Walley (2000). A survey of concepts of independence for imprecise probability. *Risk, Decision and Policy* 5, 165–181.
- Cozman, F. G. (2000a). Credal networks. *Artificial Intelligence* 120, 199–233.
- Cozman, F. G. (2000b). Separation properties of sets of probabilities. In C. Boutilier and M. Goldszmidt (Eds.), *UAI-2000*, San Francisco, pp. 107–115. Morgan Kaufmann.
- de Cooman, G., F. G. Cozman, S. Moral, and P. Walley (Eds.) (1999). *ISIPTA '99: Proceedings of the First International Symposium on Imprecise Probabilities and Their Applications*. Universiteit Gent, Belgium: The Imprecise Probability Project.
- de Cooman, G. and M. Zaffalon (2003). Updating with incomplete observations. In U. Kjærulff and C. Meek (Eds.), *Proceedings of the 19th Conference on Uncertainty in Artificial Intelligence (UAI-2003)*, pp. 142–150. Morgan Kaufmann.
- Ferreira da Rocha, J. C. and F. G. Cozman (2002). Inference with separately specified sets of probabilities in credal networks. In A. Darwiche and N. Friedman (Eds.), *Proceedings of the 18th Conference on Uncertainty in Artificial Intelligence (UAI-2002)*, pp. 430–437. Morgan Kaufmann.

- Ferreira da Rocha, J. C., F. G. Cozman, and C. P. de Campos (2003). Inference in polytrees with sets of probabilities. In U. Kjærulff and C. Meek (Eds.), *Proceedings of the 19th Conference on Uncertainty in Artificial Intelligence (UAI-2003)*, pp. 217–224. Morgan Kaufmann.
- Grunwald, P. and J. Halpern (2003). Updating probabilities. *Journal of Artificial Intelligence Research* 19, 243–278.
- Iverson, R. M., M. E. Reid, and R. G. LaHusen (1997). Debris-flow mobilization from landslides. *Annual Review of Earth and Planetary Sciences* 25, 85–138.
- Johnson, A. M. (1984). *Debris Flow*, Chapter 8, pp. 257–361. John Wiley and Sons., Ltd.
- Johnson, K. A. and N. Sitar (1990). Hydrologic conditions leading to debris flow initiation. *Can. Geotech. J.* 27, 789–801.
- Kilchenmann, U., G. Kyburz, and S. Winter (2001). *GEOSTAT user handbook*. Neuchâtel: Swiss Federal Statistical Office. In german.
- Kuntner, R. (2002). *A methodological framework towards the formulation of flood runoff generation models suitable in alpine and prealpine regions*. Ph. D. thesis, Swiss Federal Institute of Technology, Zürich.
- Levi, I. (1980). *The Enterprise of Knowledge*. London: MIT Press.
- Maidment, D. R. (1993). *Handbook of Hydrology*. McGraw-Hill.
- Moral, S. and A. Cano (2002). Strong conditional independence for credal sets. *Annals of Mathematics and Artificial Intelligence* 35(1–4), 295–321.
- Pearl, J. (1988). *Probabilistic Reasoning in Intelligent Systems: Networks of Plausible Inference*. San Mateo: Morgan Kaufmann.
- Reneau, S. L., W. E. Dietrich, C. J. Wilson, and J. D. Rogers (1984). Colluvial deposits and associated landslides in the northern San Francisco Bay area, California, USA. In *Proceedings of the IV International Symposium on Landslides*, Toronto, pp. 425–430. Canadian Geotechnical Society.
- Rinaldo, A. (1999). Hydraulic networks in nature. *Journal of Hydraulic Research* 37, 861–859.
- Takahashi, T. (1981). Debris Flow. *Ann. Rev. Fluid. Mech.* 13, 57–77.
- Takahashi, T. (1991). *Debris Flow*. Rotterdam: A.A. Balkema. IAHR Monograph.

- USDA (1993). *Soil Conservation Service*. Washington D. C.: United States Department of Agriculture. Hydrology, National Engineering Handbook, Supplement A.
- Walley, P. (1991). *Statistical Reasoning with Imprecise Probabilities*. New York: Chapman and Hall.
- Walley, P. (1996a). Inferences from multinomial data: learning about a bag of marbles. *J. R. Statist. Soc. B* 58(1), 3–57.
- Walley, P. (1996b). Measures of uncertainty in expert systems. *Artificial Intelligence* 83, 1–58.
- Wilson, R. C. and G. F. Wieczorek (1995). Rainfall threshold for the initiation of debris flows at La Honda, California. *Environ. Eng. Geosci.* 1, 11–27.